Probabilistic failure analysis of quasi-isotropic CFRP structures utilizing the stochastic finite element and the Karhunen–Loève expansion methods

Nastos, Christos; Zarouchas, Dimitrios

DOI
10.1016/j.compositesb.2022.109742

Publication date
2022

Document Version
Final published version

Published in
Composites Part B: Engineering

Citation (APA)
Nastos, C., & Zarouchas, D. (2022). Probabilistic failure analysis of quasi-isotropic CFRP structures utilizing the stochastic finite element and the Karhunen–Loève expansion methods. *Composites Part B: Engineering*, *235*, 15. Article 109742. https://doi.org/10.1016/j.compositesb.2022.109742

Composites Part B 235 (2022) 109742

Contents lists available at ScienceDirect

Composites Part B

journal homepage: www.elsevier.com/locate/composites

Probabilistic failure analysis of quasi-isotropic CFRP structures utilizing the stochastic finite element and the Karhunen–Loève expansion methods

Christos Nastos *, Dimitrios Zarouchas

Center of Excellence in Artificial Intelligence for structures, prognostics & health management, Aerospace Engineering Faculty, Delft University of Technology, Kluyverweg 1, Delft, 2629 HS, The Netherlands

Structural Integrity & Composites Group, Aerospace Engineering Faculty, Delft University of Technology, Kluyverweg 1, Delft, 2629 HS, The Netherlands

ARTICLE INFO

Keywords:
Stochastic finite element method
Karhunen–Loève expansion
Composite structures
Probabilistic methods

ABSTRACT

The accuracy of structural analysis in composite structures depends on the proper estimation of the uncertainties mainly related to the mechanical properties of the constituent materials. On this basis, a sophisticated numerical tool is proposed, able to perform stochastic finite element analysis on composite structures with material uncertainties by distributing stochastic mechanical properties along the domain of a composite structure. The output of the analysis is a probability density function for the deformation, strain, stress and failure fields. The proposed tool exploits the Karhunen–Loève expansion and the Latin Hypercube Sampling methods for the stochastic distribution of the mechanical properties, the well-established First-Order Shear Deformation theory in conjunction with a random variable approach for the calculation of stochastic stiffness matrices, and the Puck's failure criterion for the conduction of probabilistic analysis of different failure modes in composite structures. A quasi-static tensile testing campaign was conducted with quasi-isotropic coupons in order to assess the fidelity of the method and the efficiency of the stochastic distribution algorithm is compared with the full field data acquired by the digital image correlation approach. The current paper provides a thorough presentation of the development of the proposed stochastic finite element method and validation results which ensure the efficiency of the proposed stochastic numerical tool.

1. Introduction

Nowadays, composite laminates are extensively used for the design and manufacturing of lightweight and reinforced structures in the aerospace, maritime, automotive, civil construction industry, etc., due to their advantageous characteristics such as high strength, damage tolerance and light weight. The increased demand of drastic carbon emissions reduction in both the manufacturing and the transportation sectors, leads to even lighter and damage tolerant composite structures and this fact makes the design analysis more demanding. On the other hand, during the design process, the response of structures composed of fiber-reinforced composites, has shown significant deviations between numerical analysis and experimental data. The scattering response of the real-world structures is due to the inherent randomness on their mechanical properties, despite the rigorous quality checks. This means that the elimination of uncertainties due to manufacturing processes cannot be achieved, but the safety factors used since now in the structural design processes seems to lead to overweight structures which is now more critical to be encountered than before.

The finite element method (FEM) is extensively used as a trustworthy numerical tool for modeling engineering problems. The advantages of the FEM are numerous and well-known since it is a well-established method [1], however its deterministic nature enforces some limitations to describe the general characteristics of a system. This means that the FEM cannot perform reliability analysis due to the existence of uncertainties in a real-world structure. A common practice to overcome this issue is to apply safety factors in engineering design which leads to more conservative designs as already mentioned [2].

Thus, there is a need of performing probabilistic analysis including material and/or loading stochasticity and predicting the mechanical response in a probabilistic way rather than using deterministic analysis algorithms which are restricted to average values and therefore to

Abbreviations: 2D, two-dimensional; CDF, cumulative distribution function; DIC, digital image correlation; FE, finite element; FEA, finite element analysis; FEM, finite element method; FPF, first-ply-failure; FSDT, first-order deformation theory; K–L, Karhunen–Loève; LHS, latin hypercube sampling; LPF, last-ply-failure; MCS, Monte Carlo simulation; PC, polynomial chaos; PDF, probability density function; RF, random field; SFE, stochastic finite element; SFEM, stochastic finite element method

* Corresponding author.
E-mail addresses: C.Nastos@tudelft.nl (C. Nastos), d.zarouchas@tudelft.nl (D. Zarouchas).

https://doi.org/10.1016/j.compositesb.2022.109742
Received 12 December 2021; Received in revised form 27 January 2022; Accepted 11 February 2022
Available online 23 February 2022

some overestimated safety factors. In addition, the advancement of the computer science is able to accommodate the stochastic analysis, which in fact is more computationally demanding than the deterministic analysis, but can lead to more efficient designs and provide more realistic and reliable representations of the investigated structures.

A significant number of research is done for the development of reduced order methods, hyper-reduction methods and derivative driven Monte Carlo methods, which improve substantially the computational time and the feasibility of stochastic analysis [3–7]. Also, acceleration methods are reported, which enable the acceleration of the search space during sensitivity analysis or forward uncertainty quantification [8,9]. Rappel, et al. [10–12] have exploited the Bayesian inference to identify uncertain material parameters and to estimate material parameter distributions from limited/incomplete data. Deshpande et al. [13] have recently developed a Bayesian neural network for the prediction of nonlinear deformations, which shows a great potential due to the unique probabilistic predictive capabilities. On the same way, the Bayesian neural network is involved to multi-scale modeling and found that it successfully replaces local microscale solutions and overcomes the high computational cost of the direct numerical simulations [14].

The influence on the uncertainty quantification and on the reliability of the numerical models, explains the reason why computational stochastic mechanics are receiving considerable attention by the scientific community [15]. A powerful tool in computational stochastic mechanics is the stochastic finite element method (SFEM), which is an extension of the deterministic finite element (FE) approach and is able to treat random effects by modeling uncertainties during the simulation of engineering problems. Stefanou [16] has conducted a thorough state-of-art review regarding simulation methods for stochastic processes and fields, stochastic formulations and other recent developments in the area of SFEM.

Argyris et al. [17,18] have presented a stochastic formulation of a triangular shell element where the elastic modulus, the Poisson's ratio and the thickness were considered as random variables along the structural domain by applying the spectral representation method. The Monte Carlo SImulation (MCS) was exploited during this work and a large number of independent samples were generated. The MCS in conjunction with the stochastic finite element analysis (FEA) has been employed for reliability-based design optimization in shell structures where material imperfections and uncertain thickness were considered [19]. Popescu et al. [20] have exploited the combination of the MCS and FEA to study the effect of random heterogeneity of soil properties and the behavior of failure mechanisms by the prediction of stochastic shear strengths. However, the implementation of the MCS is hindered by the demanding computational effort due to the large number of samples required, thus cost effective techniques such as the Pre-conditional Conjugate Gradient Method, parallel computing etc. are needed to be investigated [21,22]. Also, other variants of the MCS have been reported to encounter the large number of samples required such as importance sampling, subset simulation and line sampling [23].

Another popular technique is the perturbation method where all the stochastic quantities are expanded around their mean value via Taylor series. This approach is limited to small perturbations and does not readily provide information on high-order statistics of the response and the resulting system of equations becomes extremely complicated beyond second-order expansion. However, the perturbation method has been reported for the development of probabilistic finite elements for structural dynamic analysis [24] and for homogenization of two phase elastic composites with random fiber and matrix elastic modulus [25]. Ding et al. [26] have presented a high order perturbation-based stochastic isogeometric method for modeling and quantifying thickness uncertainty in shell structures and the thickness randomness affect has been verified in the response of thin structures. Kamiński [27] has extended the perturbation techniques beyond its limits, in order to confirm their applicability on the inclusion of uniform and triangular probability distributions for the uncertainties of engineering problems.

Sakamoto and Ghanem [28] have presented an alternative method to generate sample functions of stochastic processes by using prescribed probability density functions (PDFs) and correlation functions and applied them into the expansion of the polynomial chaos (PC) decomposition. Field and Grigoriu [29] have examined the performance of the PC approximation in terms of accuracy and limitations by reporting some metrics; and their major findings were, that the accuracy differs from metric to metric and that the method could be computationally demanding due to the large number of coefficients that are required to be calculated. Xiu et al. [30] have exploited the polynomial chaos to develop a stochastic spectral method for modeling uncertainties in the boundary domain (rough surfaces, viscosity) in flow simulations at low Reynolds number and they proved that it outperforms the MCS method. Also Matthies and Bucher [31] have used the PC and the Hermite transform for the solution of stochastic partial differential equations which describe structures with material and geometrical random imperfections. Chen and Soares [32] have employed a spectral expansion with the use of PC to develop a stochastic finite element method for the representation of the stochastic nodal displacements in terms of normal random variables regarding laminated composite plates. The ability of the PC method to solve large deformation engineering problems has been examined and it has been observed that the performance decreases with the existence of sharp non-linearities and slope changes, hence alternative approaches are needed to be investigated [33].

On the same direction, the Karhunen–Loève expansion (K–L) has been reported in combination with the PC and the MCS for stochastic analyses and this approach is termed as spectral stochastic finite element method. In this case the random properties (mechanical, geometrical, etc.) are modeled by the K–L expansion and the probabilistic system response by the PC decomposition as well. The K–L expansion could be considered as a special case of the orthogonal series expansion, hence it is a subcase of the spectral representation methods which are able to expand the stochastic field as a sum of special functions. Grigoriu [34] has used three test applications to evaluate the K–L, spectral and sampling theorems which provide approximations for random functions by the exploitation of finite sums of deterministic functions. The evaluation of the three theorems has been conducted in terms of accuracy and limitations and both the benefits and the drawbacks are reported. Lucor et al. [35] have combined the K–L with the PC method and presented an approach to predict dynamic solutions for general random oscillators. Comparisons with the MCS method have also been presented where their proposed approach seems to outperform the MCS in terms of computational time. Schenk and Schuëller [36,37] have combined the K–L with the MCS method to study the effect of random geometric imperfections in thin-walled cylindrical shells and finally to predict the limit loads according to FE buckling analysis.

All the aforementioned stochastic techniques have been also applied for the probabilistic prediction of the mechanical response and failures in composite structures [38]. Ngah and Young [39] have combined the K–L and PC expansion to distribute random elastic properties in a unidirectional carbon fiber composite panel and to calculate the stochastic response in terms of strains as well. Their approach has been compared with the MCS and the perturbation method and it seems to be more efficient because it is applicable to a wider range of material variability than the perturbation method and it is less computational demanding than the MCS. Lin and Lam [40] have presented a method for the probabilistic failure analysis of laminated composite plates where material properties and strength parameters are treated as random variables. The phenomenological failure criterion of Tsai and Hahn was used to perform probabilistic analysis considering the first-ply-failure (FPF). Sasikumar et al. [41] have developed a SFEM using optimal linear expansion for random field discretization and the Tsai–Hill failure criterion for failure assessment of composite beams with spatially varying properties. Lal et al. [42] have combined the perturbation method and the extended finite element method to perform stochastic fracture analysis in laminated composite plates with

a central crack. Sepahvand [43] has reported a SSFEM for vibration analysis of fiber-reinforced composites with random fiber orientation and presents PDFs for the first six natural frequencies in comparison with the deterministic values obtained from the FEM. Trinh et al. [44] have presented a study aiming to quantify the stochastic buckling behavior of laminated composite plates exposed to uncertainties in material properties and lamina parameters by using the MCS for the generation of random samples. Feraboli et al. [45] have obtained the full-field strain measurements from a number of specimens via the digital image correlation (DIC) and extracted the mean values and the coefficients of variation for elastic modulus in fiber direction. By using the classic laminate plate theory, FEA and a randomization algorithm to distribute the random elastic modulus, they have generated numerically statistical distributions of full-field strains.

To the authors best knowledge, there is a limited number of papers dealing with the effects of the spatial variability of material properties and strengths on laminated composites for probabilistic failure analysis. All of these works use failure mode-independent criteria that limit the analysis to first-ply-failure. The contribution of this paper is the utilization of a failure mode-dependent criterion, i.e. Puck's failure criterion, that enables a probabilistic progressive failure analysis.

According to the aforementioned literature, the K–L expansion method is more generic than the other approaches and its advantageous functionality enables its implementation to a general purpose FE solver for conducting probabilistic structural analysis in complex structures with complicated geometries and gradients.

The present work exploits the Latin Hypercube Sampling (LHS) method and the Karhunen–Loève expansion method to generate and distribute the stochastic mechanical properties and strengths along a random field (RF). The RF is actually the mesh of the structural domain where random properties are distributed. A mapping interpolation algorithm is used to transfer stochasticity from the RF nodes to the Gaussian integration points existing on the FE mesh. The First-Order Shear Deformation theory (FSDT) for laminated composites is employed for the calculation of stochastic stiffness matrices and for the development of the proposed stochastic finite element method (SFEM). Also, the Puck's failure criterion is used for the probabilistic analysis of different matrix and fiber failure modes. To examine the validity of the proposed numerical tool, tensile experiments in quasi-isotropic coupons are conducted and the full-field strain data are extracted via the digital image correlation method. The experimental data are successfully compared with the presented stochastic numerical tool in terms of probabilistic analysis of axial strains, damage propagation and final failures.

The current article is organized as follows. Section 2 introduces the Karhunen–Loève expansion method and describes the development of stochastic finite elements with random material properties. Section 3 describes the tensile testing campaign that was conducted for the quasi-isotropic carbon fiber reinforced polymer coupons and for the material characterization as well. Section 4 presents indicative results obtained by the proposed method and correlations between numerical and experimental data regarding the probabilistic prediction of strengths.

2. Stochastic finite element for failure analysis concept

The current section presents the entire procedure followed for the development of stochastic finite elements for probabilistic failure analysis in laminated composite plates.

2.1. Spectral decomposition of random field by the Karhunen–Loève expansion

A continuous random function can be represented by a complete set of deterministic functions with corresponding random coefficients. In the general case, the spectral representation methods expand the stochastic field as a sum of trigonometric functions with random phase angles and amplitudes. Based on this idea, the K–L expansion was introduced by Spanos and Ghanem [46]. The K–L expansion can be seen as a special case of the orthogonal series expansion where the orthogonal deterministic functions, the eigenfunctions of the covariance function for the random field and the uncorrelated random variables are involved [47]. In this paper, the K–L expansion is employed for discretizing spatially varying random fields in the two-dimensional (2D) domain. Thus, both the material properties (elastic modulus, shear modulus, Poisson ratios) and the strengths (tensile, compressive) on fiber and matrix direction are decomposed into a deterministic and a stochastic part. Consider a random field $w(\mathbf{x},\theta)$ with mean value $\mu_w(\mathbf{x})$, the K–L expansion is written as [48]

$$w(\mathbf{x},\theta) = \mu_w(\mathbf{x}) + \sum_{i=1}^{\infty} \sqrt{\lambda_i}\phi_i(\mathbf{x})\xi_i(\theta) \tag{1}$$

where $\{\xi(\theta)\}_{i=1}^{\infty}$ are uncorrelated zero mean random variables and $\{\lambda_i\}_{i=1}^{\infty}$, $\{\phi_i(\mathbf{x})\}_{i=1}^{\infty}$ are the eigenvalues and eigenfunctions respectively calculated by the eigenvalue analysis of the Fredholm integral equation of the second kind, shown in Eq. (2).

$$\int_{\Omega_{2e}} C(\mathbf{x}_1;\mathbf{x}_2)\phi_k(\mathbf{x}_2)dA_{2e} = \lambda_k\phi_k(\mathbf{x}_1) \tag{2}$$

where $C(\mathbf{x}_1,\mathbf{x}_2)$ is the covariance function, A_{2e} indicates the elemental domain (Ω_{2e}) in terms of position vector $\mathbf{x}_2 = (x_2, y_2)$, that is $dA_{2e} = dx_2dy_2$. The covariance function for spatially varying random fields is constructed by Eq. (3),

$$C(\mathbf{x}_1;\mathbf{x}_2) = \sigma_w^2 exp\left(-\frac{|x_1-x_2|}{b_{c1}L_{D1}} - \frac{|y_1-y_2|}{b_{c2}L_{D2}}\right),\ \mathbf{x}_1,\mathbf{x}_2 \in \Omega \tag{3}$$

where b_{c1}, b_{c2} are the correlation length parameters of the two different directions of the domain, L_{D1}, L_{D2} are the physical characteristic lengths and σ_w is the standard deviation of the random property w. This means that the definition of random field's size is required for the calculation of Eq. (3).

The size/number of the RF elements should be selected to capture adequately the random field fluctuations of the stochastic spatial variability of the material properties. A convergence study about selecting the size of the RF field for the K–L expansion method is reported on [48] and the selected number of RF elements is recommended to satisfy the condition below:

$$N_{RF} \geq \frac{L_D}{L_c} \tag{4}$$

where L_c is the correlation length; $L_c = b_c L_D$ for each direction. Galerkin finite element techniques are used for the solution of the Fredholm integral equation (Eq. (2)) which leads to the calculation of eigenvalues and eigenfunctions [49]. According to the Galerkin finite element approach, the eigenfunction $\phi_k(\mathbf{x})$ could be expressed in a discrete domain as

$$\phi_k(\mathbf{x}) = \sum_{j=1}^{nod_{RF}} \mathbf{N}_j(\mathbf{x})d_{kj} = \langle \mathbf{N}(\mathbf{x})\rangle\{d\} \tag{5}$$

where nod_{RF} is the number of nodes per RF element, d_{kj} is the jth nodal value of the kth eigenfunction of the covariance function and $\mathbf{N}_j$ is a set of 2D shape functions. During the current work, Lagrangian interpolation shape functions are used for the formation of 9-node quadratic quadrilateral RF elements. Applying Eqs. (3), (5) into Eq. (2) leads to

$$\left[\int_{\Omega_{1e}}\int_{\Omega_{2e}} C(\mathbf{x}_1;\mathbf{x}_2)\langle \mathbf{N}(\mathbf{x}_1)\rangle^T\langle \mathbf{N}(\mathbf{x}_2)\rangle|\mathbf{J}_e|^2 dA_{2e}dA_{1e}\right]$$
$$\{d\}_e = \lambda_i \int_{\Omega_{1e}} \langle \mathbf{N}(\mathbf{x}_1)\rangle^T\langle \mathbf{N}(\mathbf{x}_1)\rangle dA_{1e}\{d\}_e \tag{6}$$

Eq. (6) denotes the integral solution for each RF element. During the total assembly of all RF elements, Eq. (6) turns into a generalized eigenvalue problem:

$$\mathbf{CD} = \mathbf{\Lambda CD} \tag{7}$$

$$\mathbf{C} = \sum_{2e=1}^{N_{RF}} \sum_{1e=1}^{N_{RF}} \int_{\Omega_{1e}} \int_{\Omega_{2e}} C(\mathbf{x}_1;\mathbf{x}_2)\langle \mathbf{N}(\mathbf{x}_1)\rangle^T \langle \mathbf{N}(\mathbf{x}_2)\rangle |\mathbf{J}_e|^2 d A_{2e} d A_{1e} \tag{8}$$

$$\mathbf{\Lambda}_{kj} = \delta_{kj}\lambda_k \tag{9}$$

$$\mathbf{B} = \sum_{e=1}^{N_{RF}} \int_{\Omega_e} \langle \mathbf{N}(\mathbf{x})\rangle^T \langle \mathbf{N}(\mathbf{x})\rangle |\mathbf{J}_e| d A_e \tag{10}$$

where $\mathbf{D}$ denotes the eigenfunction matrix and δ_{kj} is the Kronecker delta. The integration of $\mathbf{C}$, $\mathbf{B}$ matrices is achieved by the Gaussian quadrature rule. The eigenvalues analysis of Eq. (7) leads to the calculation of each nodal value of the random field $w(\mathbf{x},\theta)$ by using the truncated K–L expansion evolving M number of K–L terms.

$$w(\mathbf{x},\theta) = \mu_w(\mathbf{x}) + \sum_{i=1}^{M} \sqrt{\lambda_i}\phi_i(\mathbf{x})\xi_i(\theta) \tag{11}$$

$w(\mathbf{x},\theta)$ could be any of the randomly distributed values along the RF mesh (i.e. along the structural domain).

The random variable $\xi_i(\theta)$, actually is used to generate θ random cases by the sampling approach. The MCS is mostly used for sampling generation of different $\xi_i(\theta)$ and therefore the stochastic problem turns into θ deterministic problems. This means that the number of the required deterministic problems and as a result the computational efficiency of the stochastic method, depends on the considered sampling approach. The MCS approach is a computational demanding sampling method, because its random sampling scheme, requires a large number of samples to provide functional statistical results. This is done, because the MCS selects each random point independently from the probability distribution given for the random values. On the other hand, the Latin Hypercube sampling approach, spreads the sample points more evenly across all possible values [50]. Thus, the proposed work employs the LHS which is found to be more efficient in comparison with the MCS in terms of computational effort [51].

In the current work, elastic modulus, shear modulus, Poisson ratios, tensile and compressive strengths are treated as random values and are distributed in a stochastic way with specific mean values (μ_w) and standard deviations (σ_w) along the domain. Thus, $w(\mathbf{x},\theta)$ can be written as a vector:

$$\begin{aligned} w(\mathbf{x},\theta) = &[E_{11}(\mathbf{x},\theta)\ E_{22}(\mathbf{x},\theta)\ E_{33}(\mathbf{x},\theta)\ \upsilon_{13}(\mathbf{x},\theta)\ \upsilon_{12}(\mathbf{x},\theta) \\ &\upsilon_{23}(\mathbf{x},\theta) G_{13}(\mathbf{x},\theta)\ G_{12}(\mathbf{x},\theta)\ G_{23}(\mathbf{x},\theta)\ X_T(\mathbf{x},\theta) \\ &X_C(\mathbf{x},\theta)\ Y_T(\mathbf{x},\theta)\ Y_C(\mathbf{x},\theta)\ S(\mathbf{x},\theta)]^T \end{aligned} \tag{12}$$

where E_{11}, E_{22}, E_{33} denote the elastic modulus in principal directions 1, 2 and 3 respectively, υ_{13}, υ_{12}, υ_{23} denote the Poisson ratios in planes 13, 12 and 23 respectively, G denote the shear modulus on each of the aforementioned planes, X_T, X_C are the tensile and compressive strengths in the fiber direction, Y_T, Y_C are the tensile and compressive strengths in the matrix direction and S is the shear strength.

2.2. Mapping interpolation method

A detailed description of distributing randomly the material properties along a structural domain via the LHS and the K–L method is provided in Section 2.1. According to the described procedure, a computationally efficient random sampling of each type of property is achieved and the random values are distributed on the entire RF mesh and more specifically on the RF nodes. However, the formation of stochastic stiffness matrices and the development of stochastic finite elements (SFEs), requires the transportation of the calculated random properties from the RF field to the FE mesh.

The aforementioned process is necessary because the proposed SFEM enables the complete separation between the RF and FE mesh which is the key point to the robust stochastic modeling. The major role of the RF mesh is to distribute efficiently the stochastic variables depending on the correlation length and the M terms of the truncated K–L expansion. In this case, randomness is resulted from material heterogeneity and manufacturing processes. On the other hand, the role of the FE mesh depends on geometrical features and displacements/stress states of the structure, and is to predict converged FE solutions which are representative for real-life structures. This means that the predefined density of the two types of meshes are subjected to different criteria and the separation is beneficial, because the user can implement modifications either on the RF or on the FE mesh without affecting the convergence/performance of the other mesh type.

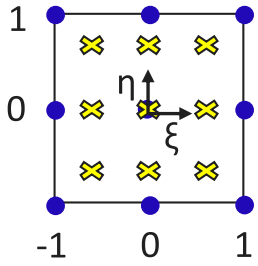

Fig. 1. The nodes and the Gaussian integration points of a 9-node quadratic quadrilateral FE. Blue dots indicate the nodes and yellow crosses indicate the integration points.

To achieve the meshes separation and finally to develop stochastic stiffness matrices; a procedure is followed to transfer the stochastic properties firstly from the RF nodes to the FE nodes and subsequently from the FE nodes to the Gaussian integration points of the FE mesh. The number and location of the Gaussian integration points depend on the selection of the shape functions or on the polynomial order. As already mentioned, the current work exploits the 9-node quadratic quadrilateral FEs both for the RF mesh and for the FE mesh. Of course, the size of the two meshes (i.e. number of elements) is different, due to the complete RF and FE mesh separation already discussed. The nodes of a 9-node FE are indicated with blue dots in Fig. 1, and the Gaussian integration points with yellow cross as well. The local coordinate system of each element (ξ,η) is placed on the center of the element. The transfer from the RF nodes to the FE nodes is achieved by transferring the eigenfunction $\phi_i(\mathbf{x})$ to the FE nodal points by using Eq. (13) below,

$$\phi_i^{jFE} = \sum_{m=1}^{9} N_m(\xi_i^j,\eta_i^j)\ \phi_m^{jRF} \tag{13}$$

where ξ_i^j, η_i^j are the isoparametric coordinates attached to the jth RF element, which correspond to the ith FE node and are calculated within each RF element. For each RF element, a nonlinear system of equations that relates the FE nodal coordinates $(x_i^j,\ y_i^j)$ within the jth RF element with the RF nodal coordinates $(X_m^j,\ Y_m^j)$ of the same jth RF element has to be solved. The nonlinear system is formulated in Eq. (14) below.

$$\begin{aligned} &\sum_{m=1}^{9} N_m(\xi_i^j,\eta_i^j)X_m^j - x_i^j = 0 \\ &\sum_{m=1}^{9} N_m(\xi_i^j,\eta_i^j)Y_m^j - y_i^j = 0 \end{aligned} \tag{14}$$

The solution of Eq. (14) and the substitution of the obtained (ξ_i^j,η_i^j) isoparametric coordinated into Eq. (13), leads to the calculation of the eigenfunction at the ith FE node within jth RF element. Thus, the random property distribution at the FE nodes can be calculated using Eq. (15), by substituting the obtained ϕ_i^{FE} from Eq. (13).

$$w^{FE}(\mathbf{x},\theta) = \mu_w(\mathbf{x}) + \sum_{i=1}^{M} \sqrt{\lambda_i}\phi_i^{FE}(\mathbf{x})\xi_i(\theta) \tag{15}$$

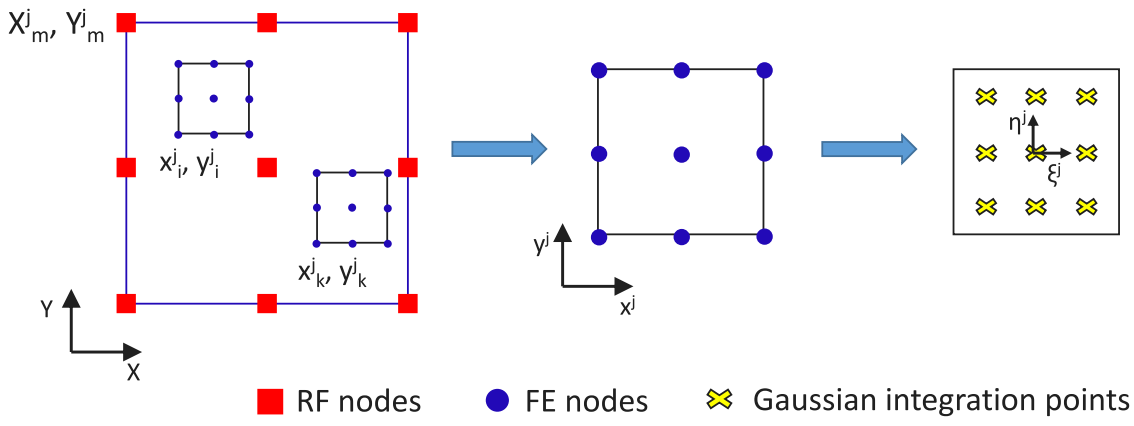

Fig. 2. The stepwise procedure for random properties transfer from RF nodes to FE nodes and from FE nodes to Gaussian integration points.

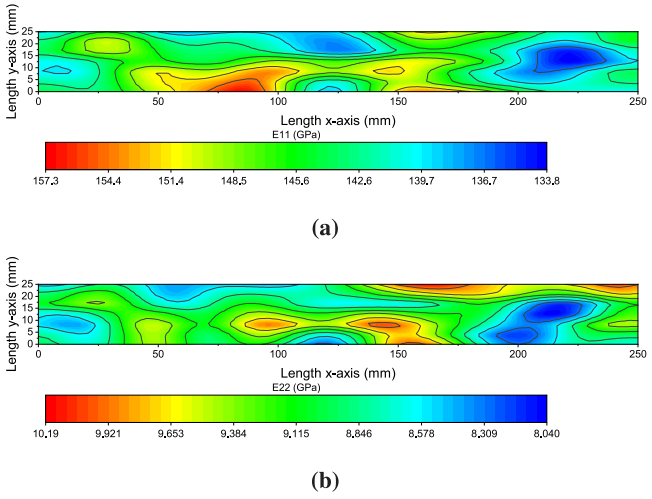

Fig. 3. Distribution of random: (a) E_{11}; (b) E_{22} mechanical properties on the Gauss integration points of the modeled structure.

The next step is to transfer the random properties from the FE nodal points to the Gaussian integration points of each FE element for the calculation of stochastic stiffness matrices by exploiting the well-established Gauss integration method. Eq. (16) describes each randomly distributed property for each θ random case,

$$w^G(\xi,\theta) = \sum_{i=1}^{9} N_i(\xi) w_i^{FE}(\mathbf{x},\theta) \tag{16}$$

where ξ are the local coordinates of the FE field (ξ^j, η^j) for the jth RF element. Fig. 2 illustrates the stepwise procedure that should be followed for the proper transfer of the desired uncertain material properties from the RF nodes to the FE nodes and subsequently from the FE nodes to the Gaussian integration points. This procedure provides the opportunity to distribute randomness to each Gauss integration point in a consistent way and subsequently enhances flexibility and precision on the calculations.

In order to illustrate some indicative results for the aforementioned procedure, Fig. 3(a) depicts the distributed E_{11} mechanical property on the Gauss integration points of a plate with dimensions 250 × 25 mm^2. The distribution is achieved by the K–L expansion method with 143.7 GPa mean value, 18.4 GPa standard deviation, 12 K–L terms and 0.1 correlation length parameters for b_{c1}, b_{c2}. On the same way, Fig. 3(b) depicts the distributed E_{22} property with 9.2 GPa mean value, 2 GPa standard deviation. All the other K–L parameters remain the same. A parametric study which considers the influence of the K–L terms and of the correlation length parameters on the random distribution is presented on Section 4.2.

2.3. Formulation of the stochastic laminated composite plate element

The current work exploits the first-order shear deformation theory [52] for the stochastic simulation of the mechanical response of laminated composite plates and the stochastic displacement field for a θ random case along x-axis, y-axis and through the thickness is described as follows:

$$\begin{aligned} u(x,y,z,\theta) &= u_0(x,y,\theta) + z\cdot\beta_x(x,y,\theta) \\ v(x,y,z,\theta) &= v_0(x,y,\theta) + z\cdot\beta_y(x,y,\theta) \\ w(x,y,z,\theta) &= w_0(x,y,\theta) \end{aligned} \tag{17}$$

where u_0, v_0, w_0 denote the stochastic displacements on the x-axis, y-axis, and z-axis at the mid-plane of the plate respectively; β_x, β_y denote the stochastic rotations of the cross-section and z is the local thickness coordinate. The in-plane strains ϵ_x, ϵ_y, ϵ_{xy} and the out of plane shear strains ϵ_{yz}, ϵ_{xz} are calculated in Eq. (18) below.

$$\begin{aligned} \varepsilon_x(x,z,\theta) &= \varepsilon_x^0(\theta) + k_x(\theta)\cdot z \\ \varepsilon_y(y,z,\theta) &= \varepsilon_y^0(\theta) + k_y(\theta)\cdot z \\ \varepsilon_{xy}(x,y,\theta) &= \varepsilon_{xy}^0(\theta) + k_{xy}(\theta) \\ \varepsilon_{yz}(y,z,\theta) &= \varepsilon_{yz}^0(\theta) \\ \varepsilon_{xz}(x,z,\theta) &= \varepsilon_{xz}^0(\theta) \end{aligned} \tag{18}$$

In the previous Eq. (18), the generalized stochastic strains of the laminated plate cross section are defined as

$$\underset{\sim}{\varepsilon_L}(\theta) = \begin{bmatrix} \varepsilon_x^0(\theta) \\ \varepsilon_y^0(\theta) \\ \varepsilon_{xy}^0(\theta) \\ k_x(\theta) \\ k_y(\theta) \\ k_{xy}(\theta) \\ \varepsilon_{yz}^0(\theta) \\ \varepsilon_{xz}^0(\theta) \end{bmatrix} = \begin{bmatrix} u_{,x}^0(\theta) \\ v_{,y}^0(\theta) \\ u_{,y}^0(\theta)+v_{,x}^0(\theta) \\ \beta_{x,x}(\theta) \\ \beta_{y,y}(\theta) \\ \beta_{x,y}(\theta)+\beta_{y,x}(\theta) \\ w_{,y}^0(\theta)+\beta_y(\theta) \\ w_{,x}^0(\theta)+\beta_x(\theta) \end{bmatrix} \tag{19}$$

where $\varepsilon_x^0, \varepsilon_y^0, \varepsilon_{xy}^0$ are implying membrane strains, k_x, k_y, k_{xy} are the curvatures and $\varepsilon_{yz}^0, \varepsilon_{xz}^0$ are the out of plain strains. The comma in the subscript indicates differentiation. The principle of virtual work for a two-dimensional solid defined in terms of axial and transverse coordinates can be recast as

$$\delta V - \delta W = 0 \tag{20}$$

where δV is the virtual strain energy and δW is the virtual work induced by external applied forces. Each of the term in Eq. (20) is given

by

$$\delta V = \int_{\Omega_0} \left\{ \int_{-h/2}^{h/2} \left[\left(\delta\varepsilon_x + z\delta k_x\right)\sigma_{xx} + \left(\delta\varepsilon_y + z\delta k_y\right)\sigma_{yy} + \left(\delta\varepsilon_{xy} + z\delta k_{xy}\right)\sigma_{xy} + \delta\varepsilon_{xz}\sigma_{xz} + \delta\varepsilon_{yz}\sigma_{yz} \right] dz \right\} dxdy = \int_{\Omega_0} \delta\underset{\sim}{\varepsilon}_L^T [\mathbf{K}_L] \underset{\sim}{\varepsilon}_L dxdy \tag{21}$$

$$\delta W = \int_{\Omega_0} \delta w_0 \left[\left(q_b + q_t\right) \right] dxdy + \int_{\Gamma_\sigma} \int_{-h/2}^{h/2} \left[\left(\delta u_n + z\delta\beta_n\right)\hat{\sigma}_{nn} + \left(\delta u_s + z\delta\beta_s\right)\hat{\sigma}_{ns} + \delta w_0 \hat{\sigma}_{nz} \right] dzds \tag{22}$$

and $\mathbf{K}_L$ is defined in Eq. (23).

$$[\mathbf{K}_L(\theta)] = \begin{bmatrix} A_{11}(\theta) & A_{12}(\theta) & A_{16}(\theta) & B_{11}(\theta) & B_{12}(\theta) & B_{16}(\theta) & & \\ A_{12}(\theta) & A_{22}(\theta) & A_{26}(\theta) & B_{12}(\theta) & B_{22}(\theta) & B_{26}(\theta) & & \\ A_{16}(\theta) & A_{22}(\theta) & A_{66}(\theta) & B_{16}(\theta) & B_{26}(\theta) & B_{66}(\theta) & & \\ B_{11}(\theta) & B_{12}(\theta) & B_{16}(\theta) & D_{11}(\theta) & D_{12}(\theta) & D_{16}(\theta) & & \\ B_{12}(\theta) & B_{22}(\theta) & B_{26}(\theta) & D_{12}(\theta) & D_{22}(\theta) & D_{26}(\theta) & & \\ B_{16}(\theta) & B_{26}(\theta) & B_{66}(\theta) & D_{16}(\theta) & D_{26}(\theta) & D_{66}(\theta) & & \\ & & & & & & A_{44}(\theta) & A_{45}(\theta) \\ & & & & & & A_{45}(\theta) & A_{55}(\theta) \end{bmatrix} \tag{23}$$

$A(\theta)'s$, $B(\theta)'s$ and $D(\theta)'s$ are the random extensional, bending and bending–extensional coupling stiffnesses for a θ random case. The approximation of the generalized strains in an elemental domain takes the form shown in Eq. (24),

$$\underset{\sim}{\varepsilon}_L(\theta) = \begin{bmatrix} \varepsilon_x(\theta) \\ \varepsilon_y(\theta) \\ \varepsilon_{xy}(\theta) \\ k_x(\theta) \\ k_y(\theta) \\ k_{xy}(\theta) \\ \varepsilon_{yz}(\theta) \\ \varepsilon_{xz}(\theta) \end{bmatrix} = \sum_{i,j=1}^{nod_{FE}} \begin{bmatrix} \boldsymbol{R}^{11} & \boldsymbol{R}^{12} & \boldsymbol{R}^{13} & \boldsymbol{R}^{14} & \boldsymbol{R}^{15} \\ \boldsymbol{R}^{21} & \boldsymbol{R}^{22} & \boldsymbol{R}^{23} & \boldsymbol{R}^{24} & \boldsymbol{R}^{25} \\ \boldsymbol{R}^{31} & \boldsymbol{R}^{32} & \boldsymbol{R}^{33} & \boldsymbol{R}^{34} & \boldsymbol{R}^{35} \\ \boldsymbol{R}^{41} & \boldsymbol{R}^{42} & \boldsymbol{R}^{43} & \boldsymbol{R}^{44} & \boldsymbol{R}^{45} \\ \boldsymbol{R}^{51} & \boldsymbol{R}^{52} & \boldsymbol{R}^{53} & \boldsymbol{R}^{54} & \boldsymbol{R}^{55} \\ \boldsymbol{R}^{61} & \boldsymbol{R}^{62} & \boldsymbol{R}^{63} & \boldsymbol{R}^{64} & \boldsymbol{R}^{65} \\ \boldsymbol{R}^{71} & \boldsymbol{R}^{72} & \boldsymbol{R}^{73} & \boldsymbol{R}^{74} & \boldsymbol{R}^{75} \\ \boldsymbol{R}^{81} & \boldsymbol{R}^{82} & \boldsymbol{R}^{83} & \boldsymbol{R}^{84} & \boldsymbol{R}^{85} \end{bmatrix} \cdot \begin{bmatrix} \hat{u}_{ij}^0(\theta) \\ \hat{\beta}_{x\,ij}(\theta) \\ \hat{v}_{ij}^0(\theta) \\ \hat{\beta}_{y\,ij}(\theta) \\ \hat{w}_{ij}^0(\theta) \end{bmatrix} \tag{24}$$

where nod_{FE} is the number of nodes per element, which depends on the choice of polynomial order for the shape functions. As stated before, the current work employs 9-node quadratic quadrilateral RF elements, therefore each element consists of 9 nodes.

$$\begin{aligned} &\mathbf{R}^{11} = \mathbf{R}^{33} = \mathbf{R}^{42} = \mathbf{R}^{64} = \mathbf{R}^{85} = N_{,x}(\xi - i)\cdot N(\eta - j) \\ &\mathbf{R}^{23} = \mathbf{R}^{31} = \mathbf{R}^{54} = \mathbf{R}^{62} = \mathbf{R}^{75} = N(\xi - i)\cdot N_{,y}(\eta - j) \\ &\mathbf{R}^{74} = \mathbf{R}^{82} = N(\xi - i)\cdot N(\eta - j) \end{aligned} \tag{25}$$

Finally, the calculation of the stochastic stiffness matrix for each element ($\mathbf{K}_e(\theta)$) is achieved in Eq. (26), by using Eqs. (23), (25) and by performing the Gauss integration method.

$$[\mathbf{K}_e(\theta)] = \iiint_V [\mathbf{R}^T][\mathbf{K}_L(\theta)][\mathbf{R}] dV \tag{26}$$

3. Experimental process

An experimental campaign was conducted both in lamina and laminate level in order to: (1) extract the material properties and the strengths on the lamina level and (2) to investigate the last-ply failures of the quasi-isotropic laminates. Several coupons are tested in both mentioned cases in order to generate population samples and finally to extract mean values and deviations of mechanical properties which actually consist the input properties to be provided to the proposed stochastic finite element (SFE).

The specimens used in the present study were manufactured from the UD carbon fiber Prepreg named Hexply® F6376C-HTS(12 K)-5%–35% with the Autoclave process. The specific Prepreg contains high tenacity carbon fibers (Tenax®-E-HTS45) and high-performance tough epoxy matrix (Hexply® 6376). The nominal fiber weight ratio and thickness of the Pregreg are 65% and 0.125 mm, respectively.

3.1. Digital image correlation apparatus

The DIC approach was employed to measure the displacement and strain distributions along the specimens field. Therefore, a pair of 5 Megapixel cameras with 23 mm lens and 75 frames-per-second was placed in the front side of the specimen, as Fig. 4 shows. Post-processing was performed using the commercial software VIC-2D® by Correlated Solutions. A subset size of 29 pixels and step size of 7 pixels were selected for correlation analysis.

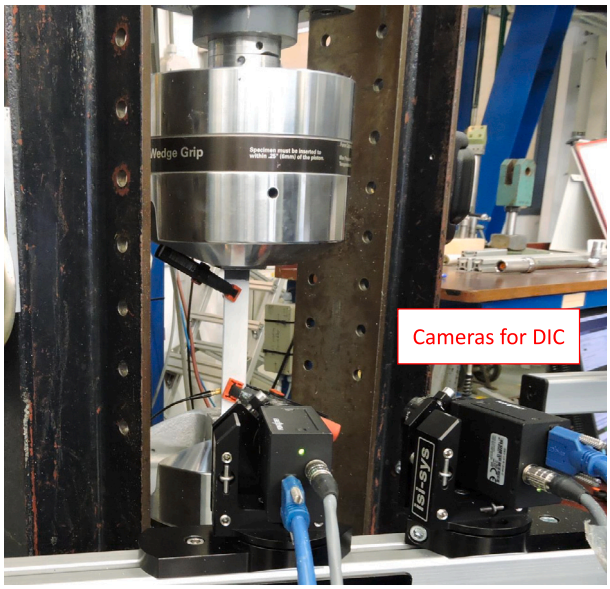

Fig. 4. A pair of 5 Megapixel cameras with 23 mm lens and 75 frames-per-second used for full-field displacements and strain measurements.

3.2. Material characterization

A set of three different tensile tests were conducted according to the relevant ASTM standards [53]: (1) on the fiber direction (0^0), (2) on the transverse direction (90^0) and (3) shear tests on the 45^0 direction. The obtained mechanical properties by the three sets of tests are the elastic modulus on the fiber direction (E_{11}), the elastic modulus on the matrix direction (E_{22}), the Poisson ratio on the 12 plane v_{12}, the shear modulus on the 12 plane G_{12}, the tensile strength on fiber (X_T) and matrix direction (Y_T) as well and the shear strength (S). The DIC approach was employed to measure displacements and strains in order to obtain the full-field distributions of the measured values for each specimen. The full-field measured distributions reveal the existence of random variability along the domain of each specimen. As an indicative example, the variability of the E_{11}, E_{22} along the specimens domain is illustrated for four arbitrarily selected specimens in Fig. 5 and Fig. 6 respectively. For both E_{11}, E_{22} cases, the elastic moduli of fiber and matrix were extracted by acquiring the strain data with DIC in the strain range between 25% and 75% and after by calculating the mean values of this range. It is observed that there are great dissimilarities along the field of each individual specimen but also between all the specimens. The same trend exists also for the rest properties. Table 1 enlists the type of mechanical properties that are extracted from the tensile tests, the number of specimens used for each property, the mean and the standard deviation value for each extracted property.

3.3. Last-ply-failure tests for the quasi-isotropic laminate

Tensile tests were also conducted to quasi-isotropic specimens for measuring the ultimate loads and strengths where the LPF exists. For that reason nine quasi-isotropic specimens were manufactured with dimensions 250 × 25 × 2 mm^3 and with lamination $[(0/90/\pm 45)_s]_2$. The loading rate of tensile machine was defined at 1 mm/min until each specimen failed.

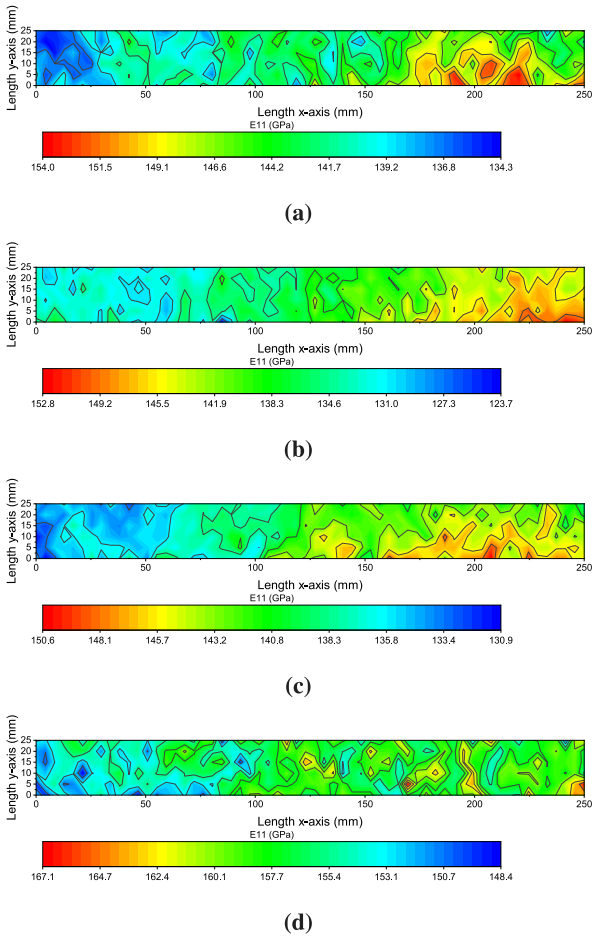

Fig. 5. The distribution of E_{11} obtained by DIC for 4 specimens. (a) Specimen 1; (b) Specimen 2; (c) Specimen 3; (d) Specimen 4.

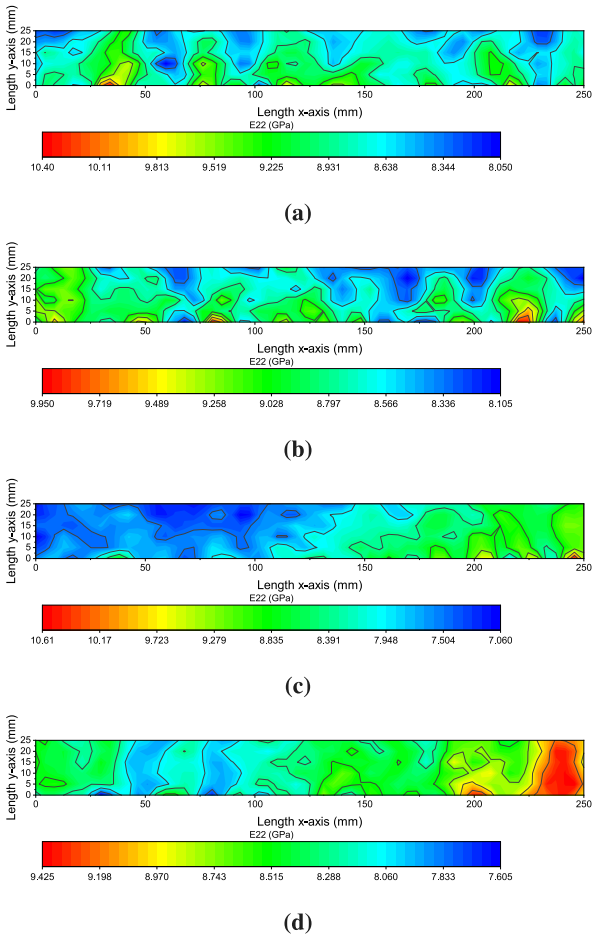

Fig. 6. The distribution of E_{22} obtained by DIC for 4 specimens. (a) Specimen 1; (b) Specimen 2; (c) Specimen 3; (d) Specimen 4.

Table 1
Mean values and standard deviations extracted by full-field DIC measurements of each specimen.

Property type (Units)	Nr. of specimens	Mean	Deviation
E_{11} (GPa)	11	143.7	18.4
E_{22} (GPa)	7	9.2	2.0
G_{12} (GPa)	5	5.1	0.7
υ_{12} (–)	11	0.37	0.14
X_T (MPa)	11	1924	146.9
Y_T (MPa)	7	107.6	9.1
S (MPa)	5	96.3	0.8

The last-ply-failure strength on the current work is assumed to exist when each specimen fails due to tensile breakage as Fig. 7 shows. Fig. 8 depicts the probability of strength (in MPa) for all the tested specimens. The lower and upper percentiles denote the confidence level bounds which were set at 95% and the reference line assumes a normal distribution for the LPF strengths with mean value of 837.0 MPa and standard deviation 19.9 MPa.

4. Results and discussion

The proposed stochastic finite element method is employed for the development of a stochastic finite element model which leads to probabilistic analysis for the different failure types that Puck's criterion encompasses, considering the quasi-isotropic specimens with lamination $[(0/90/\pm45)_s]_2$. The validity of the SFEM and its ability to conduct probabilistic failure analysis is compared with the experimental results already described in Section 3.

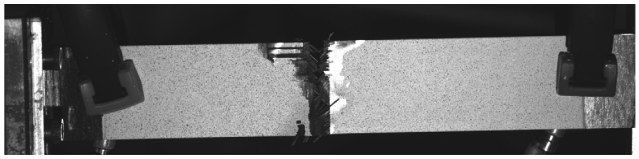

Fig. 7. Last-ply-failure of each specimen for ultimate strength measurements.

The stochastic finite element model consists of 9-node quadratic FEs, of 60×6 RF elements and of 120×12 finite elements regarding the RF and the FE mesh respectively. The model is considered as clamped on its left side and is subjected to a tensile axial load on its right edge. It has been observed via experiments that the force amplitude which is applied along the edge of each specimen variates (i.e. it is not steady) along y-axis [54]. Thus, in the current work, it is assumed that the force amplitude is variable along the right edge with $1.1F$ amplitude on the edges and with $0.9F$ on the center as shown in Fig. 9. The developed SFE can accommodate any type of load variability and that offers the opportunity to introduce uncertainties in the boundary conditions as well. The stochastic FE model is solved by progressively increasing the force amplitude until the last ply fails due to fiber tensile failure. As already discussed, the Puck's failure criterion [55] is exploited at each incremental solution for the probabilistic assessment of different failure modes.

The mechanical properties are randomly distributed using the K–L expansion with 12 K–L terms and 0.1 correlation length parameters for b_{c1}, b_{c2}. The mean values and the deviations of each property are

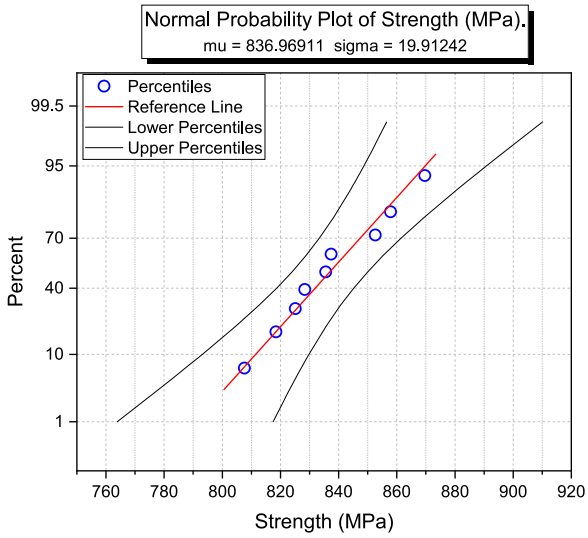

Fig. 8. Probability plot of last-ply-failure strengths (in MPa) for the 9 quasi-isotropic specimens. Normal distribution assumed within confidence level bounds of 95%. Experimental results.

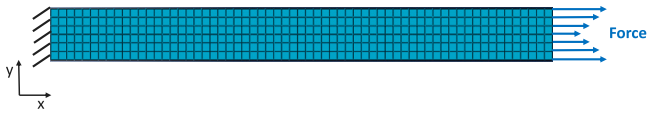

Fig. 9. A sketch of the quasi-isotropic laminate model clamped on its left side and subjected to tensile variable force on its right.

assumed to be steady along the specimen (i.e. $\mu_x(\mathbf{x}) = \overline{\mu_w}$) and the values used as an input to the K–L expansion are enlisted on Table 1. It is reported that the assumption of considering the randomness of the mechanical properties as normal distribution works properly [56] in comparison with experiments.

4.1. Selection of the number of random cases

The K–L expansion (Eq. (11)) includes the term $\xi(\theta)$ which is a random operator of θ variables with zero mean values and unit deviation. Both MCS and LHS methods could be used for generating random samples $\xi(\theta)$. The number of samples θ should be carefully selected for two main reasons: (1) in order to encompass properly the randomness of the structure and (2) to decrease the computational demand of the stochastic model. As discussed on Section 2.1, the LHS is reported to be more efficient than the MCS, hence it is employed on the proposed method. However, in order to estimate the number of θ samples that the LHS requires to generate a population of $\xi(\theta)$ values with zero mean and unit deviation, a convergence study should be conducted. The root mean square (RMS) error is used to calculate how far is the mean value of the selected θ number of samples, away from zero value which is the mean value ($\mu_w = 0$) of the required random operator $\xi(\theta)$ (Eq. (27)).

$$RMS = \sqrt{\frac{\sum_{i=1}^{\theta}(\xi(i) - \mu_w)^2}{\theta}} \tag{27}$$

Fig. 10 shows the RMS error in a logarithmic scale of the mean values of each sample number from 5 to 200 for both MCS and LHS methods. The authors assumed that a proper number of samples should achieve RMS below 0.01 ($RMS < 0.01$) and this is achieved by selecting 100 LHS method samples to generate θ values. On the other hand, the MCS needs more than 10000 samples to converge on a RMS below 0.01. Therefore, the stochastic numerical models developed during the current research, consider 100 samples generated by the LHS method.

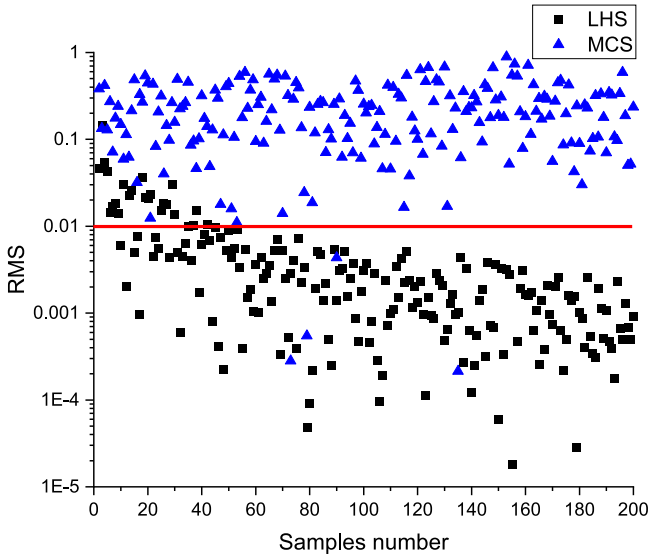

Fig. 10. RMS error of the mean values for sample numbers from 5 to 200. Convergence study comparison between the MCS and LHS methods.

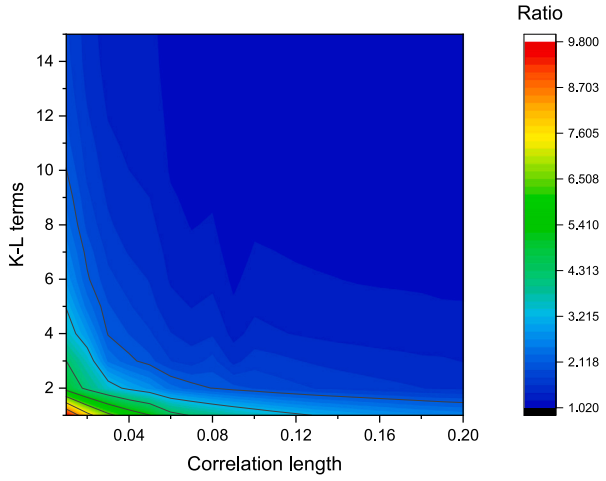

Fig. 11. Sensitivity analysis for the affect of K–L terms and correlation length on the uncertain properties distribution.

4.2. Selection of the K-L parameters

Other two parameters that should be carefully selected for the proper distribution of the uncertain properties in the material domain are the number of the K–L terms M, mentioned in Eq. (11) and the correlation length b_C mentioned in Eq. (3). A sensitivity analysis of M and b_C is conducted in order to investigate the affect of those two K–L parameters on the uncertain properties distribution. The ratio of the predefined standard deviation σ_w (Eq. (3)) to the standard deviation calculated by the obtained $w(\mathbf{x}, \theta)$ (Eq. (11)) values is used as a metric in order to estimate a functional pair of (M, b_C) values for the K–L expansion. Fig. 11 depicts the ratio values obtained by variable pairs of K–L terms and correlation lengths. It is shown that an efficient pair for the K–L expansion could be obtained from the right upper region of the contour, indicated with dark blue color. Hence, 12 K–L terms and 0.1 correlation length parameter are chosen on the current work to ensure the adequate stochastic distribution along the domain.

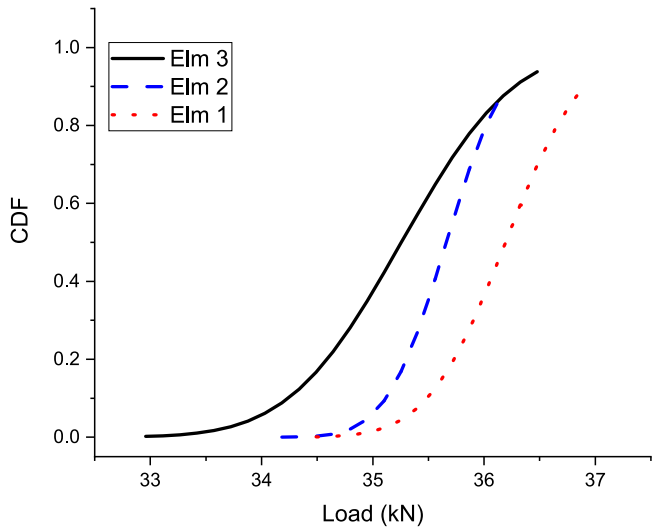

Fig. 12. CDF of the load where the inter-fiber failure mode A occurs in elements 1 (83 mm, 12.5 mm), 2 (125 mm, 16.5 mm), 3 (167 mm, 8.3 mm).

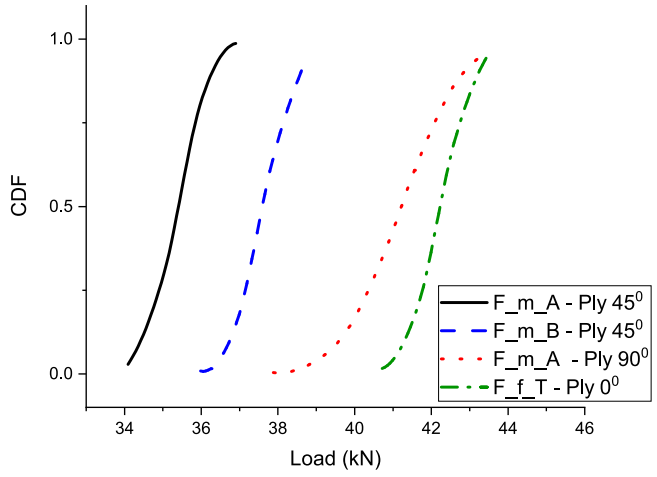

Fig. 13. Probability of matrix and fiber failures for layers $(0^0, 90^0, 45^0)$ on the central point of the quasi-isotropic plate ($x = 125$ mm, $y = 12.5$ mm).

4.3. Probabilistic analysis of failures

The current section presents indicative results for the probability of failure utilizing Puck's failure criterion in various arbitrarily selected elements by employing the proposed SFEM. For this purpose, Fig. 12 shows the cumulative distribution function of the load where the inter-fiber failure mode A (the matrix fails in tension) occurs. The CDF is illustrated for three elements with (x, y) coordinates: Elm 1 (83 mm, 12.5 mm), Elm 2 (125 mm, 16.5 mm), Elm 3 (167 mm, 8.3 mm).

Fig. 13, depicts the probabilistic progression of different type of failures that are occurred successively in different plies of the same point in the structure while tensile loading is being increased. Fig. 13 concerns the middle point of the investigated quasi-isotropic plate with (x, y) coordinates (125 mm, 12.5 mm). Firstly, the inter-fiber failure mode A on the 45^0 plies is occurred, secondly the inter-fiber failure mode B on the 45^0 plies is occurred and after that, the inter-fiber failure mode A on the 90^0 plies appears. Lastly, fiber failure under tension is occurred on the 0^0 plies. This proves that the proposed SFE model is able to provide probabilistic failure predictions for composite structures in a detailed progressive way, where the probability of each type of failure on each ply is predicted for each element of the entire domain.

Table 2
Comparison of variance values for normal, lognormal, Weibull and Gamma distribution methods. Results obtained from the experimental data.

Distribution method	Variance
Normal	396.504
Lognormal	394.849
Weibull	514.924
Gamma	371.347

4.4. Probabilistic analysis of last-ply-failures and comparisons with experimental results

In order to further examine the validity of the proposed method, probabilistic analysis of last-ply-failure is conducted and is compared with the experimental data obtained by the quasi-isotropic specimens. Different types of distributions are exploited to calculate the cumulative distributions of the experimental data. Fig. 14(a) shows the comparison of normal, lognormal, Weibull and Gamma distribution in terms of the strength values. It is observed that normal, lognormal and Gamma types of distribution are in close convergence at each other. The variance between the distributions and experimental data is quantified by the Distribution Fitter application included in the Statistics and Machine Learning Toolbox 12.0 of Matlab 2020b ©and are enlisted on Table 2.

Fig. 14(b) shows the comparison between the SFE model and the experimental results in terms of a CDF of the strengths that finally lead to FPF. A satisfactory agreement is achieved in terms of the predicted range of strength, thus the correlation with the experimental results is enough to state that the proposed method shows a great potential for probabilistic analysis in laminated composite plates.

Fig. 15 depicts the strength values and x-axis positions where last-ply-failure is occurred for each random case of the investigated quasi-isotropic composite plate models. All random cases considered in the SFE model are denoted with red circles. Regarding the predicted stochastic position, only x-axis position is depicted, because during the LPF, each specimen fails under fiber tension along its width direction (y-axis). It is observed that there are two clusters (indicated with blue circles) of random cases mostly in the range 780–830 MPa which fail near the boundaries; on the left edge where clamp exists and on the right edge where tensile load is applied. Also, during tensile experiments some specimens fail near the boundaries which is unacceptable and are excluded from the process according to ASTM standards. The same exists on the results acquired by the SFE model, which means that the proposed SFEM can predict the stochastic mechanical response in a realistic way and can conduct efficiently virtual testing in order to replace a large amount of real testings and finally to avoid cost and time effective testing campaigns.

5. Conclusions

Taking advantage of the appealing efficiency of the FEM in mechanics laminated composites and of the K–L expansion in stochastic distribution, the stochastic finite element method, has been developed and exploited for the probabilistic prediction of mechanical response and failures in laminated composite plates. The formulation of the SFEM in the context of the first-order shear deformation laminated plate theory is described.

An experimental campaign for assessing the randomness: (1) on the lamina level for each of the material property extracted and (2) on the laminate level where the strengths for the last-ply-failure were measured for the quasi-isotropic specimens, was conducted. The digital image correlation approach, has revealed the inherent randomness on lamina level and the extracted full-field values have been post-processed and the mean values, standard deviations were provided as an input to the proposed stochastic numerical tool. Five key advantages

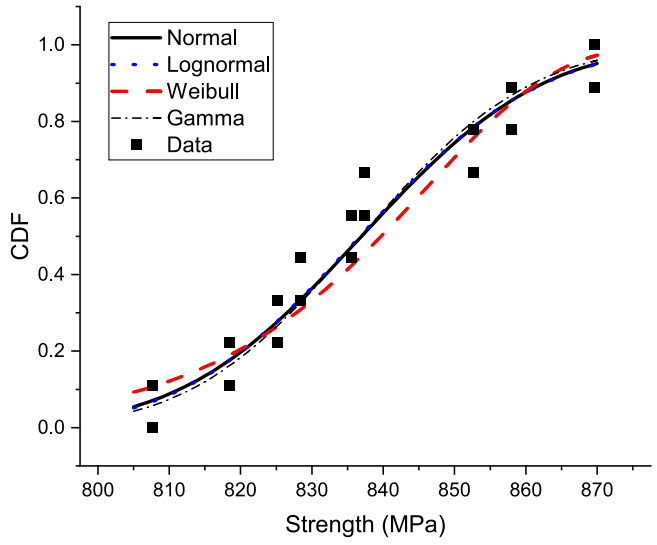

(a)

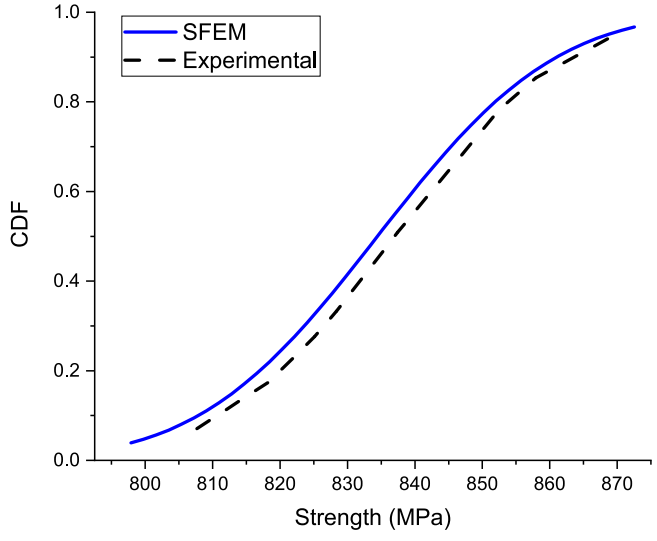

(b)

Fig. 14. (a) Experimental strength values. Comparison of normal, lognormal, Weibull and Gamma distributions; (b) Last-ply-failure. CDF comparisons between numerical and experimental data in terms of strength.

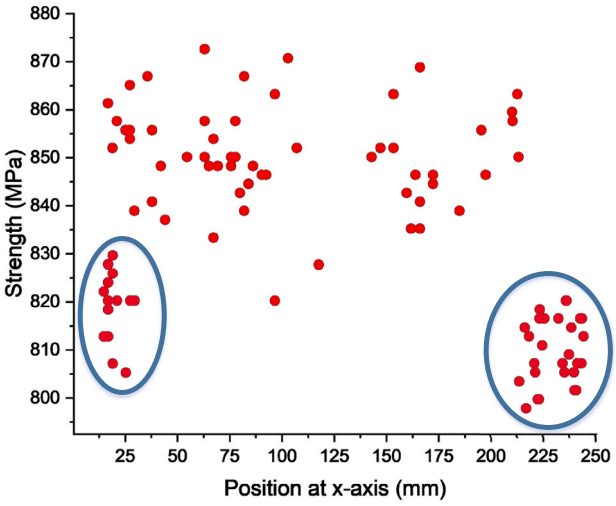

Fig. 15. Strength value and x-axis position of last-ply-failure existence for each random case (denoted with red circles).

were demonstrated: (1) the K–L expansion method can simulate efficiently the inherent randomness of composite materials and structures, (2) the LHS outperforms the MCS, since it is a "more structured" random generator and decreases the computational effort due to the smaller number of random samples required, (3) the finite element method is able to encapsulate the aforementioned stochastic schemes and to calculate stochastic discretized domains for probabilistic computational mechanics, (4) the SFEM approach performs probabilistic failure analysis on each element hence it is able to provide both holistic and detailed failure status for a composite structure, (5) the complete separation of the RF and the FE meshes increases substantially the functionality of the proposed SFEM.

In closing, the developed SFEM has shown great potential for applications in probabilistic analysis of composite structures. Future work will focus on the reliability analysis of more complex composite structures related to realistic applications, in a more detailed way since the cooperation of stochastic modeling with the FE procedures supports that.

Funding

This research did not receive any specific grant from funding agencies in the public, commercial, or not-for-profit sectors.

CRediT authorship contribution statement

Christos Nastos: Conceptualization, Methodology, Software, Validation, Data curation, Writing – original draft. **Dimitrios Zarouchas:** Conceptualization, Methodology, Writing – review & editing, Resources, Supervision.

Declaration of competing interest

The authors declare that they have no known competing financial interests or personal relationships that could have appeared to influence the work reported in this paper.

Acknowledgment

All authors approved the final version of the manuscript.

References

[1] Bathe Klaus-Jürgen. Finite element procedures for solids and structures. In: Finite Element Procedures. 1982, p. 148–214.

[2] Arregui-Mena Jose David, Margetts Lee, Mummery Paul M. Practical application of the stochastic finite element method. Arch Comput Methods Eng 2016;23(1):171–90.

[3] Ding Chensen, Deokar Rohit R, Ding Yanjun, Li Guangyao, Cui Xiangyang, Tamma Kumar K, Bordas Stéphane PA. Model order reduction accelerated Monte Carlo stochastic isogeometric method for the analysis of structures with high-dimensional and independent material uncertainties. Comput Methods Appl Mech Engrg 2019;349:266–84.

[4] Ding Chensen, Tamma Kumar K, Lian Haojie, Ding Yanjun, Dodwell Timothy J, Bordas Stéphane PA. Uncertainty quantification of spatially uncorrelated loads with a reduced-order stochastic isogeometric method. Comput Mech 2021;67(5):1255–71.

[5] Hale Jack S, Schenone Elisa, Baroli Davide, Beex Lars AA, Bordas Stéphane PA. A hyper-reduction method using adaptivity to cut the assembly costs of reduced order models. Comput Methods Appl Mech Engrg 2021;380:113723.

[6] Kerfriden Pierre, Gosselet Pierre, Adhikari Sondipon, Bordas Stephane Pierre-Alain. Bridging proper orthogonal decomposition methods and augmented Newton–Krylov algorithms: an adaptive model order reduction for highly nonlinear mechanical problems. Comput Methods Appl Mech Engrg 2011;200(5–8):850–66.
[7] Kerfriden Pierre, Goury Olivier, Rabczuk Timon, Bordas Stephane Pierre-Alain. A partitioned model order reduction approach to rationalise computational expenses in nonlinear fracture mechanics. Comput Methods Appl Mech Engrg 2013;256:169–88.
[8] Hauseux Paul, Hale Jack S, Cotin Stéphane, Bordas Stéphane PA. Quantifying the uncertainty in a hyperelastic soft tissue model with stochastic parameters. Appl Math Model 2018;62:86–102.
[9] Hauseux Paul, Hale Jack S, Bordas Stéphane PA. Accelerating Monte Carlo estimation with derivatives of high-level finite element models. Comput Methods Appl Mech Engrg 2017;318:917–36.
[10] Rappel Hussein, Beex Lars AA, Noels Ludovic, Bordas SPA. Identifying elasto-plastic parameters with Bayes' theorem considering output error, input error and model uncertainty. Probab Eng Mech 2019;55:28–41.
[11] Rappel Hussein, Beex LAA. Estimating fibres' material parameter distributions from limited data with the help of Bayesian inference. Eur J Mech A Solids 2019;75:169–96.
[12] Rappel Hussein, Beex Lars AA, Hale Jake S, Noels Ludovic, Bordas SPA. A tutorial on Bayesian inference to identify material parameters in solid mechanics. Arch Comput Methods Eng 2020;27(2):361–85.
[13] Deshpande Saurabh, Lengiewicz Jakub, Bordas Stéphane. Fem-based real-time simulations of large deformations with probabilistic deep learning. 2021, arXiv preprint arXiv:2111.01867.
[14] Krokos Vasilis, Bui Xuan Viet, Bordas Stéphane, Young Philippe, Kerfriden Pierre. A Bayesian multiscale CNN framework to predict local stress fields in structures with microscale features. Comput Mech 2021;1–34.
[15] Oden J Tinsley, Belytschko Ted, Babuska Ivo, Hughes TJR. Research directions in computational mechanics. Comput Methods Appl Mech Engrg 2003;192(7–8):913–22.
[16] Stefanou George. The stochastic finite element method: past, present and future. Comput Methods Appl Mech Engrg 2009;198(9–12):1031–51.
[17] Argyris John, Papadrakakis Manolis, Stefanou George. Stochastic finite element analysis of shells. Comput Methods Appl Mech Engrg 2002;191(41–42):4781–804.
[18] Stefanou George, Papadrakakis Manolis. Stochastic finite element analysis of shells with combined random material and geometric properties. Comput Methods Appl Mech Engrg 2004;193(1–2):139–60.
[19] Lagaros Nikos D, Papadopoulos Vissarion. Optimum design of shell structures with random geometric, material and thickness imperfections. Int J Solids Struct 2006;43(22–23):6948–64.
[20] Popescu Radu, Deodatis George, Nobahar Arash. Effects of random heterogeneity of soil properties on bearing capacity. Probab Eng Mech 2005;20(4):324–41.
[21] Charmpis Dimos C, Papadrakakis Manolis. Improving the computational efficiency in finite element analysis of shells with uncertain properties. Comput Methods Appl Mech Engrg 2005;194(12–16):1447–78.
[22] Papadopoulos Vissarion, Charmpis Dimos C, Papadrakakis Manolis. A computationally efficient method for the buckling analysis of shells with stochastic imperfections. Comput Mech 2009;43(5):687–700.
[23] Schuëller GI1168. Developments in stochastic structural mechanics. Arch Appl Mech 2006;75(10):755–73.
[24] Liu Wing Kam, Belytschko Ted, Mani A. Probabilistic finite elements for nonlinear structural dynamics. Comput Methods Appl Mech Engrg 1986;56(1):61–81.
[25] Kamiński Marcin, Kleiber Michal. Perturbation based stochastic finite element method for homogenization of two-phase elastic composites. Comput Struct 2000;78(6):811–26.
[26] Ding Chensen, Tamma Kumar K, Cui Xiangyang, Ding Yanjun, Li Guangyao, Bordas Stéphane PA. An nth high order perturbation-based stochastic isogeometric method and implementation for quantifying geometric uncertainty in shell structures. Adv Eng Softw 2020;148:102866.
[27] Kamiński Marcin. Uncertainty analysis in solid mechanics with uniform and triangular distributions using stochastic perturbation-based finite element method. Finite Elem Anal Des 2022;200:103648.
[28] Sakamoto Shigehiro, Ghanem Roger. Polynomial chaos decomposition for the simulation of non-Gaussian nonstationary stochastic processes. J Eng Mech 2002;128(2):190–201.
[29] Field Jr RV, Grigoriu M. On the accuracy of the polynomial chaos approximation. Probab Eng Mech 2004;19(1–2):65–80.
[30] Xiu Dongbin, Lucor Didier, Su C-H, Karniadakis George Em. Stochastic modeling of flow-structure interactions using generalized polynomial chaos. J. Fluids Eng. 2002;124(1):51–9.
[31] Matthies Hermann G, Bucher Christian. Finite elements for stochastic media problems. Comput Methods Appl Mech Engrg 1999;168(1–4):3–17.
[32] Chen Nian-Zhong, Soares C Guedes. Spectral stochastic finite element analysis for laminated composite plates. Comput Methods Appl Mech Engrg 2008;197(51–52):4830–9.
[33] Acharjee Swagato, Zabaras Nicholas. Uncertainty propagation in finite deformations—-A spectral stochastic Lagrangian approach. Comput Methods Appl Mech Engrg 2006;195(19–22):2289–312.
[34] Grigoriu Mircea. Evaluation of Karhunen–Loève, spectral, and sampling representations for stochastic processes. J Eng Mech 2006;132(2):179–89.
[35] Lucor Didier, Su C-H, Karniadakis George Em. Generalized polynomial chaos and random oscillators. Internat J Numer Methods Engrg 2004;60(3):571–96.
[36] Schenk CA, Schuëller GI. Buckling analysis of cylindrical shells with random geometric imperfections. Int J Non-Linear Mech 2003;38(7):1119–32.
[37] Schenk CA, Schuëller GI. Buckling analysis of cylindrical shells with cutouts including random boundary and geometric imperfections. Comput Methods Appl Mech Engrg 2007;196(35–36):3424–34.
[38] Sriramula Srinivas, Chryssanthopoulos Marios K. Quantification of uncertainty modelling in stochastic analysis of FRP composites. Composites A 2009;40(11):1673–84.
[39] Ngah MF, Young A. Application of the spectral stochastic finite element method for performance prediction of composite structures. Compos Struct 2007;78(3):447–56.
[40] Lin SC, Kam Tai-Yan. Probabilistic failure analysis of transversely loaded laminated composite plates using first-order second moment method. J Eng Mech 2000;126(8):812–20.
[41] Sasikumar P, Suresh R, Gupta Sayan. Stochastic finite element analysis of layered composite beams with spatially varying non-Gaussian inhomogeneities. Acta Mech 2014;225(6):1503–22.
[42] Lal Achchhe, Palekar Shailesh P, Mulani Sameer B, Kapania Rakesh K. Stochastic extended finite element implementation for fracture analysis of laminated composite plate with a central crack. Aerosp Sci Technol 2017;60:131–51.
[43] Sepahvand K. Spectral stochastic finite element vibration analysis of fiber-reinforced composites with random fiber orientation. Compos Struct 2016;145:119–28.
[44] Trinh Minh-Chien, Nguyen Sy-Ngoc, Jun Hyungmin, Nguyen-Thoi Trung. Stochastic buckling quantification of laminated composite plates using cell-based smoothed finite elements. Thin-Walled Struct 2021;163:107674.
[45] Feraboli Paolo, Cleveland Tyler, Stickler Patrick, Halpin John. Stochastic laminate analogy for simulating the variability in modulus of discontinuous composite materials. Composites A 2010;41(4):557–70.
[46] Spanos Pol D, Ghanem Roger. Stochastic finite element expansion for random media. J Eng Mech 1989;115(5):1035–53.
[47] Zhang Jun, Ellingwood Bruce. Orthogonal series expansions of random fields in reliability analysis. J Eng Mech 1994;120(12):2660–77.
[48] Allaix Diego Lorenzo, Carbone Vincenzo Ilario. Discretization of 2D random fields: A genetic algorithm approach. Eng Struct 2009;31(5):1111–9.
[49] Shang Shen, Yun Gun Jin. Stochastic finite element with material uncertainties: Implementation in a general purpose simulation program. Finite Elem Anal Des 2013;64:65–78.
[50] Huntington DE, Lyrintzis CS. Improvements to and limitations of latin hypercube sampling. Probab Eng Mech 1998;13(4):245–53.
[51] Olsson Anders, Sandberg Göran, Dahlblom Ola. On Latin hypercube sampling for structural reliability analysis. Struct Saf 2003;25(1):47–68.
[52] Reddy Junuthula Narasimha. Mechanics of Laminated Composite Plates and Shells: Theory and Analysis. CRC Press; 2003.
[53] ASTM Committee D-30 on High Modulus Fibers and Their Composites. ASTM Standards and Literature References for Composite Materials. Astm International; 1990.
[54] Lekou DJ, Assimakopoulou TT, Philippidis TP. Estimation of the uncertainty in measurement of composite material mechanical properties during static testing. Strain 2011;47(5):430–8.
[55] Puck A, Schürmann H. Failure analysis of FRP laminates by means of physically based phenomenological models. In: Failure Criteria in Fibre-Reinforced-Polymer Composites. Elsevier; 2004, p. 832–76.
[56] Lekou DJ, Philippidis TP. Mechanical property variability in FRP laminates and its effect on failure prediction. Composites B 2008;39(7–8):1247–56.